JOURNAL OF VIROLOGY, Mar. 1996, p. 1467–1474 Vol. 70, No. 3
0022-538X/96/$04.00+0

Attenuation Stem-Loop Lesions in the 5′ Noncoding Region of Poliovirus RNA: Neuronal Cell-Specific Translation Defects

AURELIA A. HALLER,† STACEY R. STEWART, AND BERT L. SEMLER*

Department of Microbiology and Molecular Genetics, College of Medicine, University of California, Irvine, California 92717

Received 10 July 1995/Accepted 4 December 1995

The nucleotide at position 480 in the 5′ noncoding region of the viral RNA genome plays an important role in directing the attenuation phenotype of the Sabin vaccine strain of poliovirus type 1. In vitro translation studies have shown that the attenuated viral genomes of the Sabin strains direct levels of viral protein synthesis lower than those of their neurovirulent counterparts. We previously described the isolation of pseudorevertant polioviruses derived from transfections of HeLa cells with genome-length RNA harboring an eight-nucleotide lesion in a stem-loop structure (stem-loop V) that contains the attenuation determinant at position 480 (A. A. Haller and B. L. Semler, J. Virol. 66:5075–5086, 1992). This stem-loop structure is a major component of the poliovirus internal ribosome entry site required for initiation of viral protein synthesis. The eight-nucleotide lesion (X472) was lethal for virus growth and gave rise only to viruses which had partially reverted nucleotides within the original substituted sequences. In this study, we analyzed two of the poliovirus revertants (X472R1 and X472R2) for cell-type-specific growth properties. The X472R1 and X472R2 RNA templates directed protein synthesis to wild-type levels in in vitro translation reaction mixtures supplemented with crude cytoplasmic HeLa cell extracts. In contrast, the same X472 revertant RNAs displayed a decreased translation initiation efficiency when translated in a cell-free system supplemented with extracts from neuronal cells. This translation initiation defect of the X472R templates correlated with reduced yields of infectious virus particles in neuronal cells compared with those obtained from HeLa cells infected with the X472 poliovirus revertants. Our results underscore the importance of RNA secondary structures within the poliovirus internal ribosome entry site in directing translation initiation and suggest that such structures interact with neuronal cell factors in a specific manner.

Polioviruses (PV) replicate preferentially in only a few human tissue types (for example, neuronal, gastrointestinal, oropharyngeal, and lymphoid tissues) (2, 32). A major determinant of species and tissue tropism for PV is the presence of specific receptors on the surfaces of susceptible cells (15). However, the susceptibility of specific cells to PV infection may also be influenced by additional factors (28, 34; for a review, see reference 40). Such factors may include intracellular proteins that interact with the viral genomic RNA following uncoating of virions in the cytoplasm. This RNA is a single molecule of positive (i.e., messenger sense) polarity that is ~7,400 nucleotides (nt) in length (31). The viral RNA genome has a long and extensively structured 5′ noncoding region (NCR; 742 nt for PV type 1 [PV1]) which precedes the polyprotein coding region (18, 26, 27, 29, 36). The high degree of nucleotide sequence conservation of the 5′ NCRs of the three PV serotypes suggests that this RNA segment plays an important role in the PV life cycle (39). The following are additional features of the 5′ NCR relevant to its role in virus replication. (i) The 5′ NCR harbors an internal ribosome entry site (IRES) element which mediates cap-independent translation initiation on PV RNAs (25). (ii) The complement of the 5′ NCR of PV RNA (i.e., the 3′ end of negative-strand intermediates) contains binding sites for the viral replicase and other factors involved in viral positive-strand RNA synthesis (30). (iii) A major attenuation determinant is located in the 5′ NCR of the PV genome (8, 17, 23).

For PV1, the adenine residue at position 480 in stem-loop V (also referred to as stem-loop F) of the 5′ NCR strongly influences the neurovirulence phenotype (see Fig. 1) (17). This nucleotide is changed to a guanosine residue in the Sabin type 1 strain. The resulting nucleotide substitution disrupts a highly conserved base pair and destabilizes the RNA secondary structure of the 5′ NCR of PV RNA, a structure that has been predicted on the basis of computer-generated RNA folding programs, phylogenetic comparisons, and data from biochemical probing experiments. Previous studies with PV2 and PV3, harboring the single-nucleotide alteration of the attenuation determinant at positions 481 and 472, respectively, suggested a strong correlation between the disruption of the RNA secondary structure of the 5′ NCR at this location, the neurovirulence phenotype, and viral protein synthesis (for reviews, see references 1 and 24). Evidence supporting this idea is provided by the following observations. (i) A decreased translation efficiency in vitro was observed for the attenuated PV1 and PV3 RNAs in a Krebs-2 ascites cell-free system compared with their neurovirulent counterparts (37). (ii) A cellular fraction derived from Krebs-2 ascites cells contains the initiation correction factor that stimulates the use of the correct initiation site of translation on PV RNAs. Interestingly, the initiation correction factor was less active with RNA templates from attenuated viruses than with RNAs from neurovirulent poliovirus (38). (iii) A pair of PV3 viral recombinants of attenuated and neurovirulent strains differing in nucleotide sequence only at position 472 replicated equally well in HeLa cells. However, the virus bearing the attenuating mutation at nt 472 (C→U) replicated to 10-fold-lower titers in human neuroblastoma cells

* Corresponding author. Phone: (714) 824-7573. Fax: (714) 824-8598. Electronic mail address: BLSEMLER@UCI.EDU.

† Present address: Department of Biochemistry, Biophysics, and Genetics, University of Colorado Health Sciences Center, Denver, CO 80262.

(SH-SY5Y) and was attenuated in mice. An analysis of the viral proteins present in infected cells revealed lower levels of protein synthesis directed by the attenuated virus in infected neuronal cells than the levels in infected HeLa cells (20). (iv) Macadam et al. established a correlation between the stability of the RNA secondary structure of the 5′ NCR of PV RNAs and the temperature-sensitive phenotypes of the attenuated Sabin strains (22). A genetically engineered disruption of base-paired stems in the region surrounding the attenuation determinant in stem-loop V resulted in an increase in the temperature sensitivities of the mutant viruses. In contrast, the introduction of mutations that alter the sequence but restore the stem structure had little effect on viral growth.

In this study, we analyzed PV revertants that had been previously isolated following transfection of HeLa cells with mutated, full-length viral RNA bearing a linker sequence substitution at nt 472. This site is located near a major attenuation determinant located in stem-loop V of the 5′ NCR of PV1 (12). These revertants (Se1-5NC-X472R2 and Se1-5NC-X472R1) yielded decreased levels of infectious virus in neuroblastoma cells compared with those obtained in HeLa cells. In vitro translations of the mutated RNAs bearing the X472R lesions revealed a decreased translation initiation efficiency (compared with that of wild-type RNA) in the presence of neuronal cell extracts, while differences in translation efficiency were not observed in reaction mixtures supplemented with HeLa cell extracts. In vitro-synthesized Sabin type 1 RNA templates were translated slightly less efficiently than their neurovirulent counterparts in reaction mixtures containing HeLa cytoplasmic extracts. However, the translation initiation efficiency directed by Sabin type 1 RNA was decreased significantly in cell-free reaction mixtures supplemented with neuronal cell extracts. The nucleotide sequence alterations of the X472R lesions appear to have produced RNA sequences that cannot base pair with the opposite side of a putative stem structure within stem-loop V, thereby changing the overall RNA higher-order structure that may be necessary for a functional IRES element.

MATERIALS AND METHODS

Reconstruction of the X472 and the X527 reversion mutations in subgenomic and full-length PV cDNAs. *Bsm*I fragments (~1.1 kb) from nt 456 to 1513 containing the reversion mutations of the viruses Se1-5NC-X472R1, Se1-5NC-X472R2, and Se1-5NC-X527R (described in reference 12) were generated by cDNA synthesis employing reverse transcriptase (Life Sciences) and amplification by PCR (12). The fragments were gel purified and introduced into a subclone (pT7-P1-K) of wild-type PV cDNA which contains PV sequences from nt 1 to 3064 which include the 5′ NCR and most of the P1 region of PV (6). A *Hin*dIII linker was introduced 3′ of the *Kpn*I site (nt 3064) in the PV genome. The plasmid pT7-P1-K was restricted with *Bsm*I, resulting in an ~2-kb vector fragment that was ligated to the 1.1-kb fragments harboring the X472R and X527R lesions. The plasmid DNAs were then transformed into *Escherichia coli*. The full-length PV cDNAs were constructed in the following manner: the subgenomic plasmids containing wild-type or mutant X472 sequences were digested with restriction endonuclease *Bsm*I, and the resulting 1.1-kb fragments bearing the X472R lesions were isolated. The plasmid pT7-PV1 (12) was digested with *Bsm*I, and an 8-kb DNA fragment was purified and ligated to the 1.1-kb fragments. After ligation, the cDNAs were transformed into *E. coli*, and the resulting transformants were screened for the presence of plasmids containing full-length PV cDNAs. The nucleotide sequences of the region surrounding the mutations were confirmed by DNA sequence analysis.

In vitro transcription of subgenomic PV cDNAs. The wild-type pT7-PV1 cDNA (12), pT7-PVX472 cDNA (12), and the plasmid pS1(T7)0 encoding the Sabin 1 genome (10, 16) were linearized with *Sna*BI (nt 2954), while the pT7-P1-K cDNAs (harboring the X472R and X527R mutations) were linearized with *Hin*dIII. The transcription reactions were carried out as described elsewhere (21).

Preparation of cell-free cytoplasmic extracts. HeLa S3 cells and NGP cells were grown in suspension cultures to cell densities of 5×10^5 cells per ml. The cellular cytoplasmic S10 extracts were then prepared as described previously (5, 11, 14). Prior to use in the translation reactions, the cytoplasmic extracts were treated with micrococcal nuclease (final concentration, 20 μg/ml) for 30 min at 18°C. NGP cells (human neuroblastoma cells [4, 33]) were grown in minimal essential medium supplemented with 10% fetal calf serum and 10% bovine serum (11). These cells had been adapted to growth in suspension culture from cultures of semiadherent monolayers as previously described (11). The rabbit reticulocyte lysate (RRL) was purchased from Promega.

In vitro translation of subgenomic viral RNAs. The plasmids containing PV cDNAs were linearized within the P1 region of the PV genome. In vitro transcription of the linearized cDNAs produced truncated RNAs which direct the synthesis of a single polypeptide corresponding to the capsid region of the polyprotein. The protein translated from the X472R1, X472R2, and X527R RNAs is slightly larger than the protein translated from the wild-type and X472 RNAs, since the linearization site was downstream of the *Sna*BI site used for linearization of cDNAs for synthesis of wild-type and X472 RNAs. The translation reactions were carried out as described previously (11). Subgenomic RNAs were translated in the presence of [^{35}S]methionine in RRL supplemented with cytoplasmic S10 extracts from HeLa (~15 to 20% [vol/vol]) or neuronal cells (23% [vol/vol]). Each translation reaction mixture contained 6 μg of subgenomic poliovirus RNA per ml. The translation reactions were incubated at 30°C for 3 h. RNase A was then added to a concentration of 200 μg/ml, and the incubation was continued for 20 min. After a 10-fold dilution of the reaction mixtures with Laemmli sample buffer (19), the proteins were analyzed by sodium dodecyl sulfate (SDS)–10% polyacrylamide gel electrophoresis (21). The autoradiograms of the gels were scanned with an LKB Ultrascan 2 laser densitometer.

One-step growth cycles. One-step growth analyses were carried out with wild-type PV, Se1-5NC-X472R1, and Se1-5NC-X472R2 in HeLa and NGP cells grown at 37°C in suspension cultures. The multiplicity of infection was 25. Aliquots were harvested at 1.5, 3, 4, 5.5, and 7 h postinfection and were assayed for infectious virus particle production by conducting plaque assays on confluent HeLa cell monolayers at 37°C.

Labeling of PV-infected cells with [^{35}S]methionine. HeLa or NGP cells in suspension were infected with wild-type PV, Se1-5NC-X472R1, Se1-5NC-X472R2, Se1-5NC-X527R, or Sabin type 1 PV with a multiplicity of infection of 30. At 2-h intervals, 60 μCi of [^{35}S]methionine was added to the infected cells. Two hours after addition of labeled methionine, the cells were harvested and the resulting extracts were resuspended in Laemmli sample buffer (19). The extracts were then analyzed by electrophoresis on SDS–12.5% polyacrylamide gels.

RESULTS

Characterization of the mutant X472R viruses. A previously generated linker-scanning mutation (X472), containing an 8-nt substitution within stem-loop V of the 5′ NCR of PV RNA (Fig. 1), was described as not infectious following RNA transfections in HeLa cells (12). However, this RNA was quasi-infectious (9), since pseudorevertants could be isolated, none of which contained the original 8-nt sequence substitution of X472. As shown in Fig. 1, the X472 nucleotide sequence substitution is located near a major determinant (position 480) responsible for the attenuation phenotype observed in the Sabin strain of PV1. It was of interest to determine if the X472 revertants would display growth and biosynthetic properties similar to those of the PV bearing the attenuating lesion in the 5′ NCRs of the Sabin strains. Figure 1 displays the nucleotide sequences of stem-loop V (from nt 448 to 556) of wild-type PV RNA, the original X472 mutated RNA, the RNAs isolated from the X472R1, X472R2, X527R, and the Sabin type 1 viruses. The RNA from X472R1 (resulting from RNA transfection of the mutated X472 RNA performed at 33°C) contains a single nucleotide change at position 474 (U→C) within the *Xho*I linker sequence that was introduced into the plasmid DNA that originally gave rise to the in vitro-generated X472 transcript (the RNA corresponding to the *Xho*I linker sequence is 5′-CCUCGAGG-3′). In contrast, the revertant (X472R2) recovered at 37°C has two nucleotide alterations at positions 472 (C→U) and 477 (A→C), again within the *Xho*I linker-substituted sequences. The nucleotide change at position 474 is predicted to restore a G-C base pair in stem-loop V of X472R1 RNA that was disrupted by the substituted linker sequences and resulted in a less stable G-U base pair (Fig. 1) (12). The nucleotide change at position 477 in the RNA of X472R2 is predicted to restore a G-C base present in wild-type RNA that was disrupted by the original X472 lesion. Each of

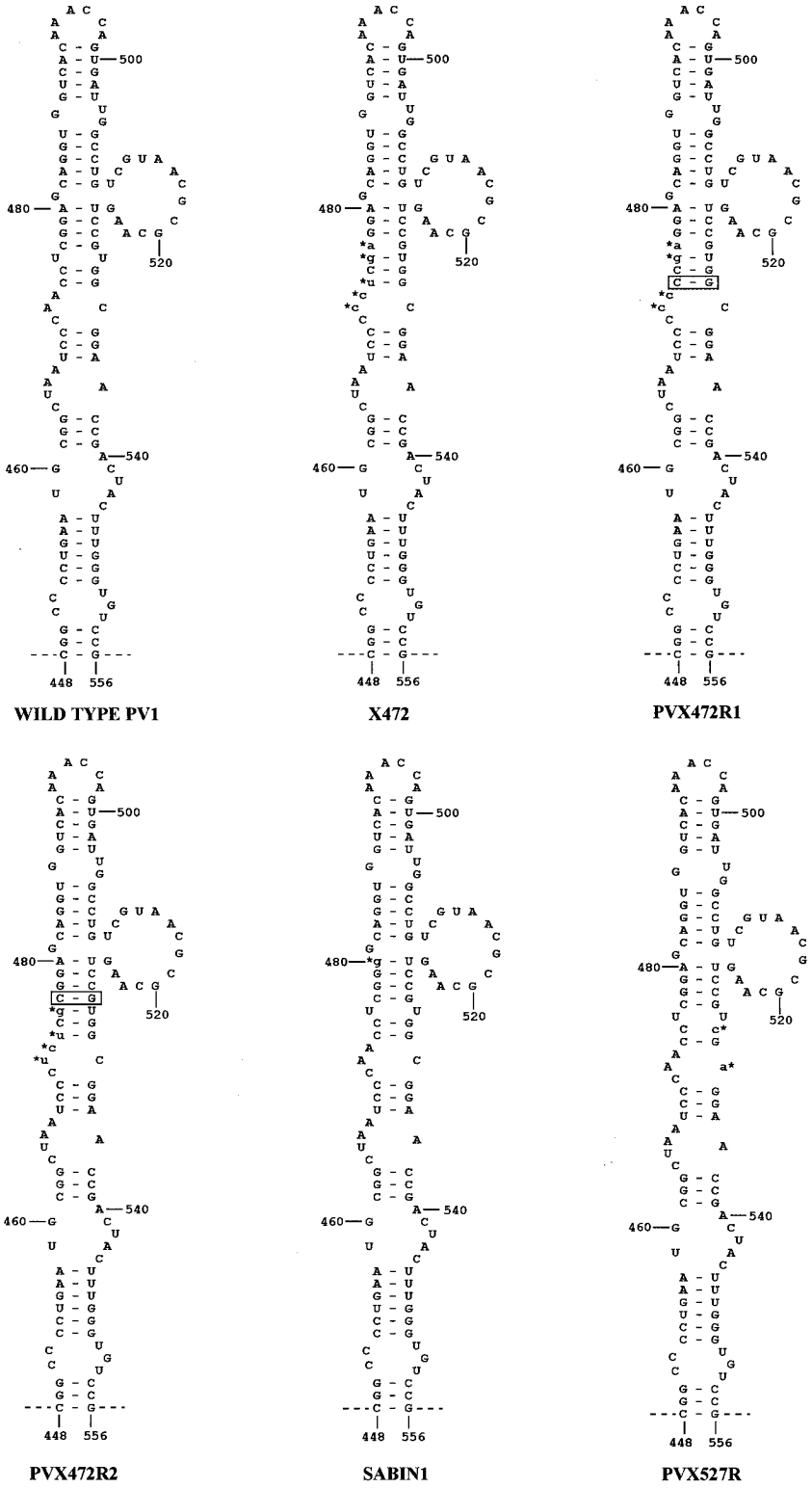

FIG. 1. Diagram of the computer-predicted RNA secondary structure of stem-loop V of the 5′ NCR of PV RNA. The numbering of the nucleotides refers to PV1. The nucleotide sequences of the wild-type PV genome, the original linker-scanning mutation (X472), the mutated RNA genomes of the PV revertants (X472R1, X472R2, and X527R), and the Sabin type 1 genome are shown. A single nucleotide is altered in the Sabin strain genome at position 480 (A→G transition). The nucleotides that differ from the wild-type PV sequence are indicated by lowercase letters with asterisks. The boxed base pairs denote changes from the X472 sequence that were found in RNAs of the R1 and R2 viruses. Note that the genomic RNA of X472R2 has an additional nucleotide change (compared with the original X472 lesion), a C→U transition at nt 472 that is not predicted to form a base pair.

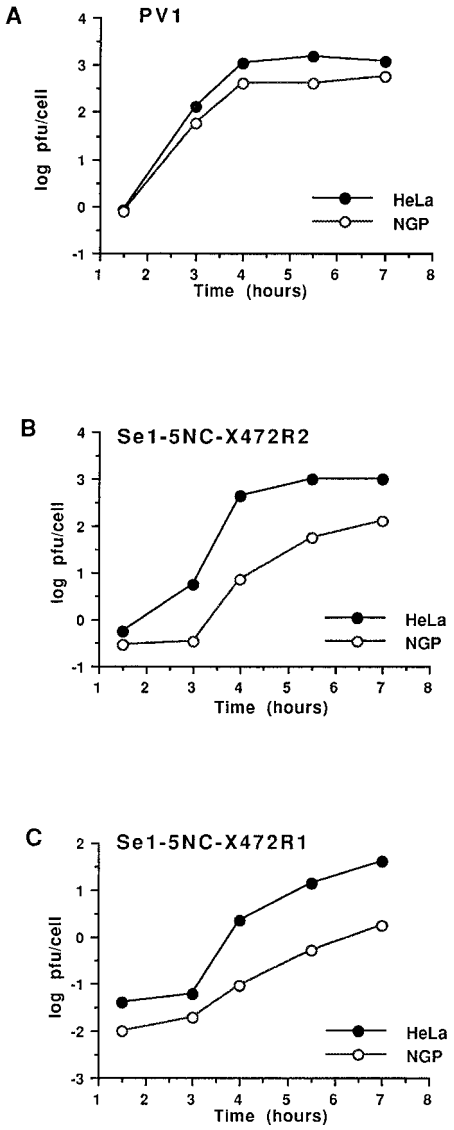

FIG. 2. One-step growth analysis of wild-type virus (A) and Se1-5NC-X472R2 (B) and Se1-5NC-X472R1 (C) mutant viruses in HeLa cell and NGP cell suspension cultures at 37°C. HeLa cells or neuronal cells were infected with the mutant and wild-type viruses at a multiplicity of infection of 25. At the indicated times, an aliquot of infected cells was harvested. The samples were analyzed for infectious virus particle formation via plaque assays.

the X472 revertants contains a total of four nucleotide alterations in the 5′ NCRs of their RNA genomes. The sequences within the targeted region of stem-loop V for both X472 revertants are predicted to still form the same number of base pairs as the RNA sequences for wild-type virus, but two of these are energetically less favorable G-U base pairs not present in the wild-type RNA sequence (Fig. 1).

We also employed a different revertant, Se1-5NC-X527R, that contains a sequence substitution on the opposite side of the predicted base-paired region of stem-loop V that was perturbed by the X472 mutations (Fig. 1) (12). Se1-5NC-X527R was isolated upon RNA transfections of the mutated X527 RNA in HeLa cells at 37°C. The X527 RNA was derived from a plasmid containing an 8-nt *Xho*I linker substitution in cDNA sequences beginning at position 527 within the PV1 5′ NCR. Virus isolated from transfection of this RNA into HeLa cells at 33°C was temperature sensitive for growth at 39°C, whereas virus isolated from transfections carried out at 37°C was not temperature sensitive and gave rise to the X527R isolate. Upon nucleotide sequence analysis, the viral RNA isolated from X527R-infected HeLa cells was shown to contain a single nucleotide change at position 528 (C→G) within the *Xho*I linker sequence. This substitution would be predicted to allow the formation of a base pair. Interestingly, in PV1, the guanosine at position 528 is predicted to base pair with the cytidine at position 477, the same position of a reversion identified for the X472R2 isolate (described above). The conservation of this particular base pair in two different viral revertants suggests that the stability of this stem structure is important for viral functions.

A cDNA segment corresponding to a small region of the 5′ NCRs of the revertant viruses (harboring the X472R lesions or the X527R lesion) was generated by reverse transcription-PCR amplification (RT-PCR) and introduced into a plasmid containing a cDNA copy of the wild-type PV1 genome to ensure the absence of second-site reversions at other locations in the viral genome. The full-length, mutated cDNAs were transcribed in vitro, and the resulting RNAs were transfected into HeLa cells. The reconstructed X527R virus revertant displayed a small-to-medium plaque size and was used in in vivo protein-labeling experiments (described below). Both of the reconstructed X472R1 and X472R2 revertants displayed small plaque phenotypes in HeLa and neuronal cells. A one-step growth analysis was carried out at 37°C by infecting HeLa or neuronal cells (NGP) with the X472R viruses (Fig. 2). Wild-type PV produced the same levels of infectious particles at 37°C in both HeLa cells and NGP cells (Fig. 2A). In contrast, Se1-5NC-X472R2 exhibited an ~1-log-unit-reduced virus yield (Fig. 2B), and Se1-5NC-X472R1 displayed a decrease of ~1.5 log units in the titer of infectious virus particles in NGP cells compared with the titer in HeLa cells (Fig. 2C). Se1-5NC-X472R1 appeared to be slightly growth impaired, as revealed by the ~1.5-log unit reduction of infectious virus produced in HeLa cells compared with wild-type virus (compare peak virus yields in Fig. 2B with those in Fig. 2C).

In vitro translation efficiencies of the mutated subgenomic RNAs. To determine whether the differential growth phenotypes of the Se1-5NC-X472R1 and Se1-5NC-X472R2 viruses observed in HeLa and NGP cells were correlated with reduced translation efficiencies of the mutated RNAs, in vitro translations were carried out (as described in Materials and Methods). Mutated and wild-type RNAs truncated in the P1 coding region of the PV genome were assayed in vitro in a cell-free translation system (RRL) alone or were supplemented with a HeLa cell or neuroblastoma cell cytoplasmic extract (Fig. 3). The subgenomic RNAs of the PV genome produce a single polypeptide which facilitates the quantitation of the translation efficiencies of the RNA templates. The translation products were analyzed on SDS–10% polyacrylamide gels, and the autoradiograms were scanned with a laser densitometer to obtain a quantitative analysis (Table 1). The levels of translation initiation observed with wild-type mRNAs were arbitrarily set at 100%, and the levels observed for the mutated RNAs represent a fraction thereof. In the translation reaction mixtures supplemented with HeLa cell cytoplasmic extract, the X472R1 and X472R2 RNAs and the X527R RNAs were translated as efficiently as wild-type mRNAs (Fig. 3A, lane 3 and lanes 5 to 7). As reported previously, RNAs harboring the original X472 lesion were translated in HeLa cell extract-supplemented reactions at levels that were only ~3 to 5% of those observed for wild-type mRNAs (Fig. 3A, lane 4) (12). Interestingly, when the same RNA templates were translated in reaction mixtures

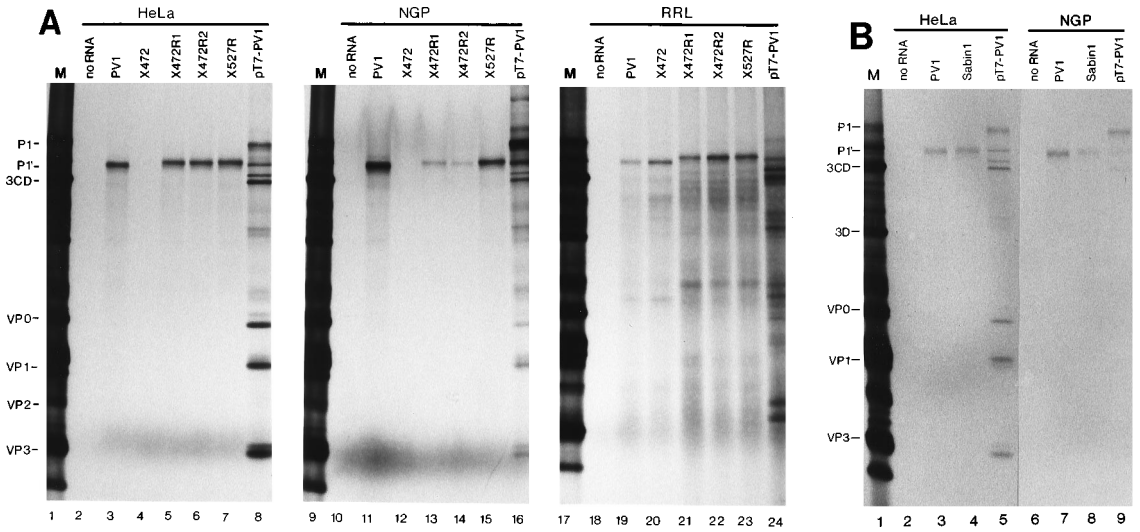

FIG. 3. (A) In vitro translation of subgenomic transcripts of wild-type PV (PV1), X472, X472R1, X472R2, and X527R in cell-free reaction mixtures supplemented with HeLa or neuronal cell extracts or in RRL alone. Lanes 2 to 8 show the translation reaction mixtures supplemented with HeLa cell cytoplasmic extract (18% [vol/vol]). Lanes 10 to 16 depict the reaction mixtures to which neuronal cytoplasmic extract was added (23% [vol/vol]), and lanes 19 to 24 show the translation efficiencies of these RNAs in RRL alone. no RNA, translation reaction mixtures without RNA (lanes 2, 10, and 18); pT7-PV1, translation reaction mixtures containing full-length PV RNA (lanes 8, 16, and 24). Radiolabeled PV proteins were used as markers (lanes 1, 9, and 17). (B) In vitro translation of subgenomic transcripts of wild-type and Sabin type 1 RNAs in reaction mixtures containing HeLa or neuronal (NGP) cytoplasmic extracts. Lanes: 3 and 4, in vitro translation reaction mixtures supplemented with cellular extracts from HeLa cells (18% [vol/vol]); 7 and 8, the levels of translation efficiency in the presence of neuronal cell extracts (23% [vol/vol]); 5 and 9, full-length wild-type RNAs translated in the presence of HeLa and NGP extracts, respectively. no RNA, RNA not added to the translation reactions. [^{35}S]methionine-labeled PV proteins are marked on the left side of the panel. P1′, the truncated P1 translation product.

supplemented with cytoplasmic extracts derived from neuronal cells, quite different results were obtained. The X472 RNAs directed translation at a low efficiency (3 to 5% compared with wild-type levels) in the reaction mixtures supplemented with neuronal extracts (Fig. 3A, lane 12). However, the mutated RNAs containing the X472R nucleotide reversions showed a dramatic decrease in translation initiation efficiency in the cell-free system supplemented with neuronal cell extracts compared with reaction mixtures containing HeLa cell extracts (Fig. 3A, lanes 13 and 14). The X472R1 RNAs were translated to levels that were ~23% of those observed for wild-type mRNAs, while the X472R2 RNAs directed translation initiation to levels that were ~12% of those observed for wild-type templates. The mutated X527R RNAs directed translation only slightly less efficiently in NGP extracts (~80%) compared with wild-type RNAs (Fig. 3A, lane 15). Interestingly, the Sabin type 1 RNAs translated at ~70% of the levels observed for wild-type RNAs in the reaction mixtures supplemented with HeLa cell extract (Fig. 3B, lanes 3 and 4). In the reaction mixtures supplemented with extracts from neuronal cells, the translation efficiencies of the Sabin type 1 RNAs were reduced to 30% of wild-type levels (Fig. 3B, lanes 7 and 8). These results suggested that the X472R templates interact with the translation apparatus of neuronal cells in vitro in a fashion similar to that of attenuated RNA templates from attenuated viruses.

TABLE 1. Translation efficiencies of wild-type and mutated RNAs in a cell-free system supplemented with HeLa cell or NGP cytoplasmic extracts

RNA template	Efficiency[a]	
	HeLa S10	NGP S10
PV1	100	100
X472[b]	<5	<5
X472R1	100	23
X472R2	100	12
X527R	100	80
Sabin type 1	67	32

[a] Autoradiograms were quantitated by laser densitometric scanning, and the translation levels of wild-type PV RNA were arbitrarily set at 100%.
[b] Not infectious.

In contrast to the above observations, the levels of translation initiation of all RNA templates in RRL alone appeared to be very inefficient (Fig. 3A, lanes 19 to 23, and Fig. 3B, lanes 10 and 11). It should be noted that the polyacrylamide gels resulting from electrophoretic separations of the protein products of the translations in RRL were exposed to film three times longer than those derived from the HeLa or NGP translations. Multiple aberrant internal translation products were visible for all RNAs, as has been reported previously (7, 11). Interestingly, the X472 RNAs that were not translated efficiently in the reaction mixtures supplemented with HeLa or NGP extracts displayed levels of translation initiation similar to those of wild-type RNAs, demonstrating a lack of translation stimulating and/or mRNA discriminatory factors in the RRL. These results suggest that viral RNAs bearing lesions in a region of the 5′ NCR implicated to play a role in the attenuation phenotype (between positions 470 to 481) can differentially interact with the neuronal cytoplasmic factors to result in decreased levels of viral protein synthesis.

Mutant viral protein synthesis in infected HeLa and NGP cells. The kinetics of mutant viral protein synthesis in HeLa cells or NGP cells infected with Se1-5NC-X472R1, Se1-5NC-X472R2, or Se1-5NC-X527R were analyzed. We also included control infections with wild-type PV1 or Sabin type 1. [^{35}S]methionine was added to infected cells (incubated at 37°C) at specific intervals, after which the cells were harvested, resuspended in Laemmli sample buffer, and analyzed on an SDS–12.5% polyacrylamide gel. In Fig. 4A and B, lanes 1 to 3 show the patterns of protein synthesis produced in HeLa cells or

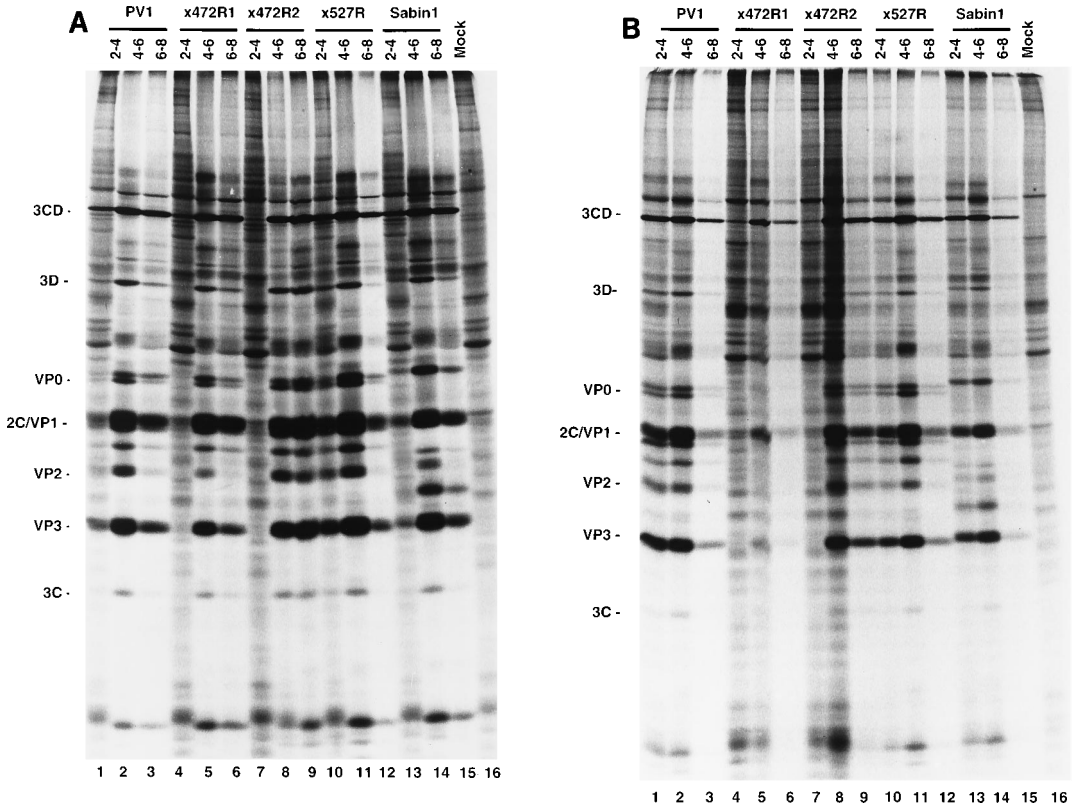

FIG. 4. [^{35}S]methionine-labeled proteins from cells infected with wild-type, Se1-5NC-X472R1, Se1-5NC-X472R2, Se1-5NC-X527R, and Sabin 1 viruses. HeLa (A) or neuroblastoma (B) suspension cultures were infected with the wild-type or mutant viruses at a multiplicity of infection of 30. After adsorption, the infected cell cultures were pelleted and resuspended in methionine-free modified Eagle medium (plus 10% fetal calf serum and 25 mM *N*-2-hydroxyethylpiperazine-*N*′-2-ethanesulfonic acid [HEPES; pH 7.4]) and incubated at 37°C. At 2, 4, and 6 h postinfection, 60 μCi of [^{35}S]methionine was added for 2 h, after which the cells were harvested and resuspended in Laemmli sample buffer. The labeled proteins were analyzed on an SDS-12.5% polyacrylamide gel. MOCK, HeLa (A) or neuroblastoma (B) cells that were mock infected and harvested 4 h postinfection. The PV proteins are indicated to the left of each panel.

NGP cells, respectively, infected with wild-type PV. The production of viral proteins in NGP cells infected with the X472 revertants was significantly delayed compared with their production in HeLa cells infected with either X472R1 or X472R2. Protein synthesis levels in NGP cells infected by wild-type PV peaked at 4 to 6 h postinfection (lane 2), while those in NGP cells infected with the X472R1 virus never reached the same peak seen for wild-type virus (compare lane 2 with lane 5 in Fig. 4B). In NGP cells infected with the X472R2 virus, the appearance of viral proteins was delayed compared with that of cells infected with wild-type PV1 (compare Fig. 4B, lane 7 and lane 1); however, accumulation of viral proteins reached levels comparable to those of wild-type virus by the 4- to 6-h time point (Fig. 4B, compare lanes 8 and 2). In a control experiment with a virus whose genomic RNA directed in vitro translation to nearly wild-type levels, HeLa cells and NGP cells infected with the Se1-5NC-X527R virus exhibited the same kinetics of viral protein synthesis as that detected for wild-type virus (lanes 10 to 12 in Fig. 4A and B). Interestingly, the Sabin type 1 virus directed the synthesis of viral proteins in infected NGP cells to levels nearly equivalent to those of wild-type virus (Fig. 4B, lanes 13 to 15 and lanes 1 to 3).

Neither of the X472 revertants inhibited host cell protein synthesis in NGP cells as efficiently as wild-type PV (compare the 4- to 6-h time points for all three viruses, Fig. 4B). Since the 2A proteinase is involved in host cell shutoff (for a review, see reference 13), the complete nucleotide sequences of the 2A regions of both X472R viruses were analyzed. The nucleotide sequence of the 2A region for both X472R viruses was found to be wild type (data not shown). Thus, other determinants of the X472 viral revertants must be responsible for the observed defect in the shutoff of host cell protein synthesis. One such determinant may be the delayed onset of viral protein synthesis that results in overall decreased levels of 2A proteinase.

DISCUSSION

PV revertants bearing lesions in their RNA genomes near a major attenuation determinant were analyzed for their growth properties in different cell types. Both X472 revertants (isolated at 33 and 37°C) originate from X472 RNA transfections of HeLa cells, and their genomes deviate from the wild-type RNA sequence by only 4 nt located in stem-loop V of the 5′ NCR (Fig. 1). A virus containing the original X472 mutation was not isolated. Interestingly, the nucleotide changes present in the X472 revertants occurred in the introduced linker sequence such that additional base pairs could form (with respect to the original X472 mutation). A different PV revertant, Se1-5NC-X527R, contains a single nucleotide change in the introduced linker sequence on the opposite side of the stem-loop structure, such that an additional base pair can form (with respect to the original X527 RNA) in the same stem structure that is affected by the X472 lesion. These observations suggest that the stability of the RNA secondary structure of stem-loop V is crucial for viral functions (12). Previous studies showed that RNAs of attenuated PV3 replicated to 10-fold-lower titers in

cells of neuronal origin compared with HeLa cells (20). Thus, the growth properties of the two PV revertants, Se1-5NC-X472R1 and Se1-5NC-X472R2, were investigated by carrying out a one-step growth analysis in HeLa cells and in neuronal cells (NGP). The Se1-5NC-X472R2 virus grew as efficiently as wild-type PV in HeLa cells. However, this revertant displayed an ~1-log unit reduction of infectious virus yield in neuronal cells. In addition, the yield of infectious virus produced by the X472R1 virus in neuronal cells was reduced by 1.5 log units compared with the yield in HeLa cells.

Svitkin et al. observed a reduced translation initiation efficiency of RNA templates containing attenuating lesions compared with that of RNA from neurovirulent viruses in Krebs-2 ascites cell extracts (37). Lower levels of virus proteins were also observed in neuronal cells infected with an attenuated PV3 recombinant compared with those produced in infected HeLa cells (20). The above studies suggested that viral protein synthesis plays a role in the attenuation phenotype of PV. Thus, it was of interest to determine the levels of translation initiation directed by the RNAs from the X472 revertant viruses in vitro in a cell-free system supplemented with cytoplasmic extracts from either HeLa cells or neuronal cells. Indeed, the X472R mutated RNA templates directed translation initiation as efficiently as wild-type mRNAs in reaction mixtures containing HeLa cell extract. However, a dramatic reduction in the translation initiation efficiency of the X472R1 and X472R2 RNAs was observed in the reaction mixtures supplemented with neuronal cell extracts (~10 to 25% of the levels observed for wild-type mRNAs). In contrast, RNA from the X527R virus was translated at nearly wild-type levels in a cell-free system, independently of the type of cellular extract added. Interestingly, the Sabin type 1 RNAs translated less efficiently (~70%) than wild-type RNAs in RRL supplemented with HeLa cytoplasmic extracts, and their efficiency of translation initiation was even further reduced in the reaction mixtures containing neuronal extracts (~30% of the levels observed for wild-type mRNAs). These data show that the RNAs from the X472 PV revertants direct protein synthesis in vitro at levels similar to those produced by RNAs isolated from the attenuated Sabin strains.

The accumulation of viral proteins observed in vivo in NGP cells infected with the mutant viruses (X472R1 and X472R2) resulted in the expected array of virus structural and nonstructural proteins but was delayed compared with wild-type virus. The effects on translation appeared to be cell type specific, since both X472R1 and X472R2 infections of HeLa cells led to the accumulation of viral proteins during the course of an infection with kinetics nearly identical to those of wild-type PV. These in vivo findings, coupled with the observed delay in shutoff of host cell protein synthesis in NGP cells infected with either X472R1 or X472R2, are consistent with the extract-specific translation defects seen in the in vitro translation experiments (Fig. 3; Table 1). However, we cannot rule out the possibility that the X472R1 and X472R2 viruses are also somewhat defective in functions such as RNA replication or virion assembly. Data have been reported which suggest that the IRES element of the PV1 5′ NCR contains determinants that affect viral RNA replication (3). Recently, Nomoto and coworkers (35) have uncovered a cell-type-specific determinant in the 5′ NCR of the PV genome that exerts its effect on viral RNA synthesis. Thus, it remains to be determined if the cell-specific growth defects displayed by the X472 revertant viruses are solely due to effects on translation initiation.

The data presented in this study suggest that the RNAs derived from the X472R1 and X472R2 viruses interact with the translation apparatus present in neuronal cells in a manner comparable to that of the attenuated RNA templates. Thus, the X472 revertants represent a unique system to study the complex effects of attenuating mutations mapping to the IRES sequences because these viruses have neuronal cell-specific defects in translation that are even more pronounced than those of the Sabin type 1 attenuated strain. The X472R RNAs harbor a 4-nt sequence substitution in stem-loop V of the 5′ NCR, resulting perhaps in a less stable secondary or higher-order structure conformation. Stem-loop V of the 5′ NCR is proposed to be an integral part of the IRES element of PV RNAs (11, 12, 25). Therefore, the nucleotide changes in stem-loop V of the X472R RNAs may affect the conformation of the IRES, resulting in lower levels of translation initiation on viral RNAs. Alternatively, the altered nucleotide sequences of the X472 revertants may not influence the overall RNA structure of the IRES element. Rather, the altered sequences present in the RNAs from the X472 revertants and the attenuated viral genomes generate a binding site for a negatively acting factor found only in neuronal cells. This RNA-protein interaction may then be responsible for the reduced levels of viral protein synthesis observed. It is also conceivable that the sequence changes may alter a binding site that is normally occupied by a factor that is limiting in neuronal cells compared with its levels in HeLa cells. The lack of this RNA-protein interaction with stem-loop V sequences of PV RNA may result in the observed decreased translation initiation efficiencies. To determine which of these models is correct, a biochemical approach resulting in the fractionation of cytoplasmic extracts derived from both HeLa and neuronal cells will be required. The obtained fractions can then be assayed for their abilities to stimulate cap-independent translation initiation on wild-type and mutated X472R RNA templates. Further, it will be of interest to test the X472R viruses for their neurovirulence potential in transgenic mice expressing the human cell receptor necessary for PV attachment. Ultimately, this experimental approach should yield information that will help to unravel the role of translation initiation in the attenuation/neurovirulence phenotype of PV.

ACKNOWLEDGMENTS

We thank Jonathan Towner for critical reading of the manuscript. We are grateful to Akio Nomoto for the vector pS1(T7)0 encoding the Sabin type 1 cDNA. We also thank Hung Nguyen for his assistance and his scientific expertise.

This work was supported by Public Health Service grant AI26765. A.A.H. and S.R.S. were supported by predoctoral traineeships from the National Institutes of Health (GM07134 and AI07319, respectively).

REFERENCES

1. **Agol, V. I.** 1990. Current approaches to the problem of poliovirus attenuation, p. 311–318. *In* M. A. Brinton and F. X. Heinz (ed.). New aspects of positive-strand RNA viruses. American Society for Microbiology, Washington, D.C.
2. **Bodian, D.** 1955. Emerging concept of poliomyelitis infection. Science **12:** 105–108.
3. **Borman, A. M., F. G. Deliat, and K. M. Kean.** 1994. Sequences within the poliovirus internal ribosome entry segment control viral RNA synthesis. EMBO J. **13:**3149–3157.
4. **Brodeur, G. M., G. S. Sekhon, and M. N. Goldstein.** 1977. Chromosomal aberrations in human neuroblastomas. Cancer **40:**2256–2263.
5. **Brown, B. A., and E. Ehrenfeld.** 1979. Translation of poliovirus RNA *in vitro*: changes in cleavage pattern and initiation sites by ribosomal salt wash. Virology **97:**396–405.
6. **Dildine, S. L., K. R. Stark, A. A. Haller, and B. L. Semler.** 1991. Poliovirus translation initiation: differential effects of directed and selected mutations in the 5′ noncoding region of viral RNAs. Virology **182:**742–752.
7. **Dorner, A. J., B. L. Semler, R. J. Jackson, R. Hanecak, E. Duprey, and E. Wimmer.** 1984. In vitro translation of poliovirus RNA: utilization of internal initiation sites in reticulocyte lysate. J. Virol. **50:**507–514.
8. **Evans, D. M. A., G. Dunn, P. D. Minor, G. C. Schild, A. J. Cann, G. Stanway,**

J. W. Almond, K. Currey, and J. V. Maizel, Jr. 1985. Increased neurovirulence associated with a single nucleotide change in a non-coding region of the Sabin type 3 poliovaccine genome. Nature (London) **314:**548–550.
9. **Gmyl, A. P., E. V. Pilipenko, S. V. Maslova, G. A. Belov, and V. I. Agol.** 1993. Functional and genetic plasticities of the poliovirus genome: quasi-infectious RNAs modified in the 5′-untranslated region yield a variety of pseudorevertants. J. Virol. **67:**6309–6316.
10. **Hagino-Yamagishi, K., and A. Nomoto.** 1989. In vitro construction of poliovirus defective interfering particles. J. Virol. **63:**5386–5392.
11. **Haller, A. A., J. H. C. Nguyen, and B. L. Semler.** 1993. Minimum internal ribosome entry site required for poliovirus infectivity. J. Virol. **67:**7461–7471.
12. **Haller, A. A., and B. L. Semler.** 1992. Linker scanning mutagenesis of the internal ribosome entry site of poliovirus RNA. J. Virol. **66:**5075–5086.
13. **Haller, A. A., and B. L. Semler.** 1995. Translation and host cell shutoff, p. 113–133. *In* H. A. Rotbart (ed.), Human enterovirus infections. American Society for Microbiology, Washington, D.C.
14. **Helentjaris, T., E. Ehrenfeld, M. L. Brown-Luedi, and J. W. B. Hershey.** 1979. Alterations in initiation factor activity from poliovirus-infected HeLa cells. J. Biol. Chem. **254:**10973–10978.
15. **Holland, J. J.** 1961. Receptor affinities as major determinants of enterovirus tissue tropisms in humans. Virology **15:**312–326.
16. **Iizuka, N., M. Kohara, K. Hagino-Yamagishi, S. Abe, T. Komatsu, K. Tago, M. Arita, and A. Nomoto.** 1989. Construction of less neurovirulent polioviruses by introducing deletions into the 5′ noncoding sequence of the genome. J. Virol. **63:**5354–5363.
17. **Kawamura, N., M. Kohara, S. Abe, T. Komatsu, K. Tago, M. Arita, and A. Nomoto.** 1989. Determinants in the 5′ noncoding region of poliovirus Sabin 1 RNA that influence the attenuation phenotype. J. Virol. **63:**1302–1309.
18. **Kitamura, N., B. L. Semler, P. G. Rothberg, G. R. Larsen, C. J. Adler, A. J. Dorner, E. A. Emini, R. Hanecak, J. J. Lee, S. van der Werf, C. W. Anderson, and E. Wimmer.** 1981. Primary structure, gene organization, and polypeptide expression of poliovirus RNA. Nature (London) **291:**547–553.
19. **Laemmli, U. K.** 1970. Cleavage of structural proteins during the assembly of the head of bacteriophage T4. Nature (London) **227:**680–685.
20. **La Monica, N., and V. R. Racaniello.** 1989. Differences in replication of attenuated and neurovirulent polioviruses in human neuroblastoma cell line SH-SY5Y. J. Virol. **63:**2357–2360.
21. **Lawson, M. A., B. Dasmahapatra, and B. L. Semler.** 1990. Species-specific substrate interactions of picornavirus 3C proteinase suballelic exchange mutants. J. Biol. Chem. **265:**15920–15931.
22. **Macadam, A. J., G. Ferguson, J. Burlison, D. Stone, R. Skuce, J. W. Almond, and P. D. Minor.** 1992. Correlation of RNA secondary structure and attenuation of Sabin vaccine strains of poliovirus in tissue culture. Virology **189:**415–422.
23. **Nomoto, A., M. Kohara, S. Kuge, N. Kawamura, M. Arita, T. Kamatsu, S. Abe, B. L. Semler, E. Wimmer, and H. Itoh.** 1987. Study on virulence of poliovirus type 1 using *in vitro* modified viruses, p. 437–452. *In* M. A. Brinton and R. R. Rueckert (ed.), Positive-strand RNA viruses. Alan R. Liss, Inc., New York.
24. **Nomoto, A., and E. Wimmer.** 1987. Genetic studies of the antigenicity and the attenuation phenotype of poliovirus. Symp. Soc. Gen. Microbiol. **40:**107–134.
25. **Pelletier, J., and N. Sonenberg.** 1988. Internal initiation of translation of eukaryotic mRNA directed by a sequence derived from poliovirus RNA. Nature (London) **334:**320–325.
26. **Pilipenko, E. V., V. M. Blinov, L. I. Romanova, A. N. Sinyakov, S. V. Maslova, and V. I. Agol.** 1989. Conserved structural domains in the 5′-untranslated region of picornaviral genomes: an analysis of the segment controlling translation and neurovirulence. Virology **168:**201–209.
27. **Racaniello, V. R., and D. Baltimore.** 1981. Molecular cloning of poliovirus cDNA and determination of the complete nucleotide sequence of the viral genome. Proc. Natl. Acad. Sci. USA **78:**4887–4891.
28. **Ren, R., and V. R. Racaniello.** 1992. Human poliovirus receptor gene expression and poliovirus tissue tropism in transgenic mice. J. Virol. **66:**296–304.
29. **Rivera, V. M., J. D. Welsh, and J. V. Maizel.** 1988. Comparative sequence analysis of the 5′ noncoding region of the enteroviruses and rhinoviruses. Virology **165:**42–50.
30. **Roehl, H. H., and B. L. Semler.** 1995. Poliovirus infection enhances the formation of two ribonucleoprotein complexes at the 3′ end of viral negative-strand RNA. J. Virol. **69:**2954–2961.
31. **Rueckert, R. R.** 1991. Picornaviridae and their replication, p. 409–450. *In* B. N. Fields and D. M. Knipe (ed.), Fundamental virology, 2nd ed. Raven Press, New York.
32. **Sabin, A. B.** 1956. Pathogenesis of poliomyelitis: reappraisal in light of new data. Science **123:**1151–1157.
33. **Schwab, M., K. Alitalo, K.-H. Klempnauer, H. E. Varmus, J. M. Bishop, F. Gilbert, G. Brodeur, M. Goldstein, and J. Trent.** 1983. Amplified DNA with limited homology to myc cellular oncogene is shared by human neuroblastoma cell lines and a neuroblastoma tumour. Nature (London) **305:**245–248.
34. **Shepley, M. P., and V. R. Racaniello.** 1994. A monoclonal antibody that blocks poliovirus attachment recognizes the lymphocyte homing receptor CD44. J. Virol. **68:**1301–1308.
35. **Shiroki, K., T. Ishii, T. Aoki, M. Kobashi, S. Ohka, and A. Nomoto.** 1995. A new *cis*-acting element for RNA replication within the 5′ noncoding region of poliovirus type 1 RNA. J. Virol. **69:**6825–6832.
36. **Skinner, M. A., V. R. Racaniello, G. Dunn, J. Cooper, P. D. Minor, and J. W. Almond.** 1989. New model for the secondary structure of the 5′ non-coding RNA of poliovirus is supported by biochemical and genetic data that also show that RNA secondary structure is important in neurovirulence. J. Mol. Biol. **207:**379–392.
37. **Svitkin, Y. V., S. V. Maslova, and V. I. Agol.** 1985. The genomes of attenuated and virulent poliovirus strains differ in their *in vitro* translation efficiencies. Virology **147:**243–252.
38. **Svitkin, Y. V., T. V. Pestova, S. V. Maslova, and V. I. Agol.** 1988. Point mutations modify the response of poliovirus RNA to a translation initiation factor: a comparison of neurovirulent and attenuated strains. Virology **166:** 394–404.
39. **Toyoda, H., M. Kohara, Y. Kataoka, T. Suganuma, T. Omata, N. Imura, and A. Nomoto.** 1984. Complete nucleotide sequences of all three poliovirus serotype genomes: implication for genetic relationship, gene function, and antigenic determinants. J. Mol. Biol. **174:**561–585.
40. **Wimmer, E., J. J. Harber, J. A. Bibb, M. Gromeier, H.-H. Lu, and G. Bernhardt.** 1994. Poliovirus receptors, p. 101–127. *In* E. Wimmer (ed.), Cellular receptors for animal viruses. Cold Spring Harbor Laboratory Press, Cold Spring Harbor, N.Y.